Romanian Journal of Petroleum & Gas Technology
Vol. VI (LXXVII) • No. 2/2024

NUMERICAL MODELING OF THERMAL ENERGY TRANSFER BETWEEN ROCKS AND GROUNDWATER

Ioana Purghel [1], Maria Stoicescu [2*], Dragos Cristea [2], Monica Tegledi [3]
[1] Doctoral School (Mines, Oil and Gas), Petroleum-Gas University of Ploiesti, Romania
[2] Faculty of Oil and Gas Engineering, Petroleum-Gas University of Ploiesti, Romania
[3] Economical Science Faculty, Petroleum-Gas University of Ploiesti, Romania
* e-mail (corresponding author): stoicescu.maria@yahoo.com

DOI: 10.51865/JPGT.2025.02.05

ABSTRACT

Geothermal energy, derived from the Earth's internal heat, stands out as a powerful and consistent renewable resource. Unlike intermittent sources such as solar and wind, it provides a stable, 24/7 baseload power supply suitable for everything from large-scale electricity generation to direct-use heating and climate control. This study investigates the low-enthalpy geothermal potential near the Petroleum-Gas University of Ploiesti, Romania, where the ground maintains a constant temperature of 13-14°C at a 100-meter depth. We developed a numerical model to simulate the heat transfer between rock formations and groundwater to assess the viability of a thermal recovery project.The simulation results point to a stable heat transfer rate of 2-10 kW/m² from the surrounding rock to the groundwater. Our model shows that a four-well system could sustainably produce water at 13.5°C with a flow rate of 30 l/h over a 10-year period, causing a negligible temperature drop of less than 0.5°C in the reservoir. Ultimately, the model confirms that harnessing low-enthalpy geothermal energy in Ploiesti is a viable option. The constant and accessible underground temperature presents a significant opportunity for direct-use applications, such as a district heating system for the university campus. This research demonstrates that even modest thermal gradients can be effectively utilized to develop local and sustainable energy solutions.

Keywords: thermal rocks, ANNs model, environment simulation, geothermal energy, numerical simulation, pollution analysis

INTRODUCTION

Unlike renewable sources dependent on the sun, such as solar or wind energy, geothermal energy is a direct manifestation of the Earth's internal dynamics.

The source of this energy is twofold. First is primordial heat, the residual thermal energy from the planet's violent formation 4.5 billion years ago, which is still stored in the Earth's core where temperatures exceed 5000°C, [1].

Second is radiogenic heat, a continuous process where radioactive isotopes like uranium, thorium, and potassium naturally disintegrate within the Earth's crust and mantle, generating about 50% of the total heat reaching the surface, [2].

Together, these sources produce a constant heat flux of approximately 44.2 TW radiating from the planet's interior, [3].

The fact that the Earth continuously produces its own heat gives geothermal energy a major advantage: sustainability on a geological scale, [4].

While fossil fuels are finite and other renewables depend on short-term cycles like day/night or seasons, the geothermal resource is constant, [5].

Harnessing this constant, low-temperature energy is a key strategy for institutions aiming to decarbonize their heating and cooling systems, [6].

An example of this approach is the project undertaken by the Petroleum-Gas University of Ploiesti [7].

In line with national and European energy commitments, the university initiated a project in 2020 to modernize its campus energy infrastructure by implementing a hybrid, modular system for renewable energy generation (Figure 1).

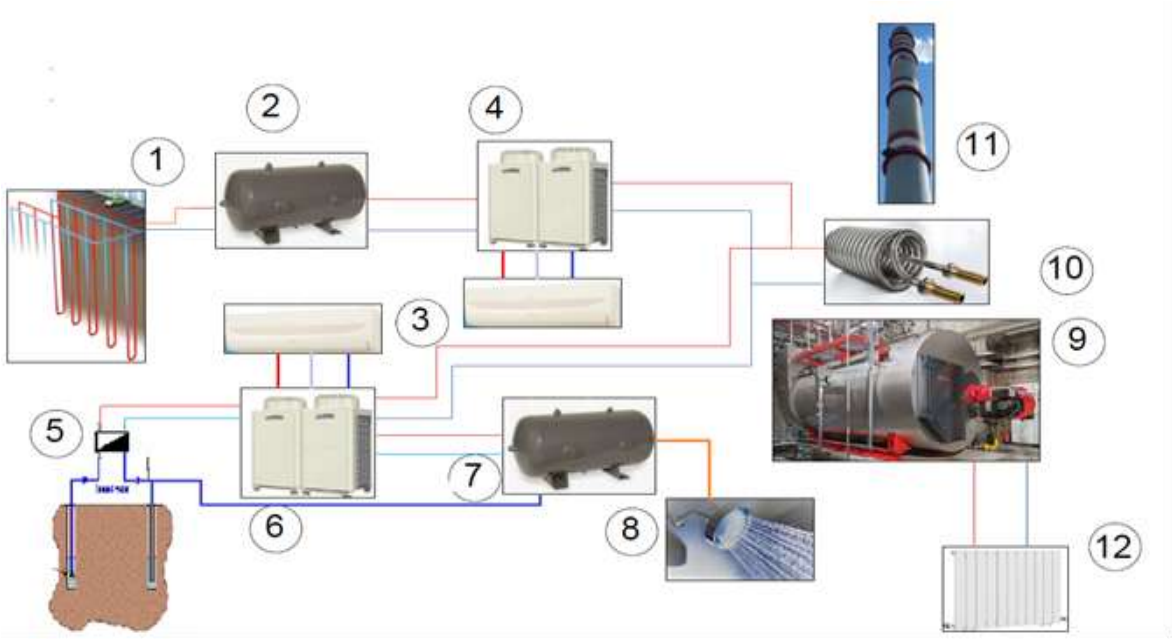

Figure 1. *Hybrid system for improving energy efficiency* [7]*:*

1 – closed ground heat exchanger, new, 2 – storage tank, new, 3 – fan coil units, new, 4 – heat pumps with double ground-water heat exchanger, new, 5 – water wells, new, 6 - water-water heat pumps, new, 7- hot water tanks campus, old, 8 – hot water showers, old, 9– heating boilers, old, 10 – boiler stack heat recovery, new, 11 - boiler stack, old 12 - current campus radiators, old

The core of this project is an integrated energy solution based on heat pump technology, designed to cover the campus's baseload heating requirements and significantly reduce natural gas consumption and associated emissions [8].

The system utilizes both water-to-water and ground-to-water heat pumps, supported by a network of extraction and reinjection wells drilled into the local multi-layered aquifer system.

The hydrogeological potential of the area is confirmed by the presence of major groundwater bodies with high transmissivity, [9].

However, the project's long-term success is contingent upon navigating the complex and variable local hydrogeology.

Initial studies revealed a non-homogeneous subsurface with multiple aquifer horizons, making it difficult to predict the thermal performance and sustainability of the geothermal wells, [10].

This geological uncertainty presents a significant challenge for efficient system management. Therefore, the primary objective of this paper is to develop a numerical model that simulates the thermal transfer processes between the rock formations and the groundwater.

This study aims to evaluate the efficiency of the geothermal extraction system and to assess its long-term impact on the subsurface thermal regime, thereby ensuring the project's sustainability. The developed system is a unitary energy solution, designed to increase the energy efficiency of the campus. Based on heat pump technology, the system is sized to cover the basic requirements, with the objectives of reducing the consumption of fossil fuels (natural gas) and polluting emissions generated by the current facilities.

The study area is located within the Ploiești municipality, which overlies groundwater bodies of regional importance: ROIL18 (Teleajen Alluvial Cone) and ROAG12 (Eastern Wallachian Depression). These formations confirm the high hydrogeological potential of the area, with filtration coefficients ranging from 50-150 m/day and transmissivities between 500–2000 m²/day, [11].

Geophysical investigations, including electrometry up to a 100 m depth, and data from boreholes revealed a complex and variable geological structure. This variability makes it difficult to delineate a continuous, homogeneous aquifer.

Hydrogeological studies have identified three primary aquifer horizons:

1. *Shallow Phreatic Aquifer*: Found in Quaternary deposits (sands, gravels) at a depth of up to 8-10 m. It has a low flow rate (approx. 1.3-1.5 l/s per well) and is vulnerable to surface pollution.
2. *Deep Aquifer*: Located at 42-52 m within fractured Oligocene-Miocene deposits.
3. *Pressurized Aquifer*: A confined layer at a depth of 78-92 m within permeable sand layers of Middle Pleistocene age.

The project involved the installation of a hybrid geothermal and heat recovery system. To ensure the necessary flow rate of approximately 30 l/s for the heat pumps, four water extraction and exploitation boreholes were drilled.

The system consists of the following main components:

- 6 water-to-water heat pumps, supplied by a system of 4 extraction wells and 3 reinjection wells.
- 4 ground-to-water heat pumps, which utilize closed-loop geothermal wells.
- 3 heat recovery units, installed on the exhaust stacks of the university's existing natural gas boilers.

The overall engineering approach was designed to ensure that the system operates in full compliance with all relevant national and EU standards.

METHODS AND ANALYSIS

The analysis of energy transfer from the rock formations to the extracted groundwater was conducted in two main stages.

The first stage focused on the thermal properties of groundwater contaminated with petroleum products, a common issue in the Ploiesti drilling area. Our methodology assumes that remediation is a prerequisite for geothermal operations. We, therefore, simulated the reduction of the contaminant plume through the extraction of polluted groundwater.

This decontamination process was modeled using the following concentration depletion equation, [12]:

$$C(t) = C_0 e^{-\lambda t} + N(\mu, \sigma^2) \quad (1)$$

where:

$C(t)$- represents the pollutant concentration at time *t*,

C_0 is the initial concentration,

λ represents the decrease constant (decontamination rate), set as a function of the pollutant concentration in each well,

t represents the decontamination time (hours),

$N(\mu, \sigma^2)$ is the residual pollution.

The second relationship that analyzes groundwater thermals around an annual average is, [13]:

$$T(t) = T_{medie} + A \sin(\frac{2\pi t}{24}) + N(\mu, \sigma^2) \quad (2)$$

where:

$T(t)$ is the layer temperature at time *t*,

T_{medie} represents the multiannual temperature,

A is the amplitude of the daily temperature variation.

In the analysis of the evolution of strata thermality we used AI (Machine Learning) because it is necessary to evaluate the energy costs and the quantities of water needed to be extracted to reduce pollution.

AI models using in this analyis is expressed by the equations, [14]:

- **Liniar Regresion Model**

$$\hat{y} = \beta_0 + \beta_1 x_1 + \beta_2 x_2 \quad (3)$$

The purpose of this linear regression model is to train the equations to find optimal values for the coefficients β and $\hat{y}$ is the predicted value of the pollutant concentration, β_0 is the free term (the intercept) and defines the prediction value when all variables are equal to zero, β_1 and β_2 are the coefficients (weights) that the model uses to describe its prediction $\hat{y}$ for a change with a corresponding unit for x_1 and x_2.

- **The Decision Tree Model**

Is represented by a single equation, the prediction being given by the space of input variables which is divided into disjoint rectangular regions R_1, R_1,... R_1,.

The mathematical equation of the prediction AI is of the form, [15]:

$$\hat{y} = f(x) = \sum_{m=1}^{M} c_m \quad I(x \in R_m) \quad (4)$$

The model defines thresholds such as if the time required to decontaminate the layer and the layer temperature is then the prediction is.

In the equation above M is the number of terminal regions (leaves of the tree), R_m is the m-th region analyzed, c_m is the constant value for the region R_m and represents the average of the target values (concentration) for the model training points and $I(x \in R_m)$ is an indicator function that if m is 1 then the point x belongs to the region R_m and if it is zero then it is not part of the analysis.

- **Random Forest Regressor Model**

This model is an assembly of decision trees, its equation being a subset of the data, [16].

$$\hat{y} = \frac{1}{B}\sum_{b=1}^{B} f_b(x) \quad (5)$$

In the equation of this model B is the total number of decision trees in the forest and $f_b(x)$ is the prediction of the b-th decision tree.

The model is robust and less prone to errors (than a single decision tree).

- **Gradient Boosting Regressor**

It is an additive and sequential data assembly model. Each new tree is trained to correct the errors (residuals) of the model formed from all previous trees, [17].

The model is built iteratively and works on the following analysis system, [18]:

a. Start with an initial prediction (usually with target values $F_0(x) = \bar{y}$.
b. For each iteration (tree) from 1 to M, the errors of the previous model are calculated: $r_{im}(x) = y_i - F_{m-1}(x_i)$.
c. Train a new decision tree $h_m(x)$ to predict the errors (residuals),
d. Update the total model by adding a new tree, weighted by a learning rate v,

$$F_m(x) = F_{m-1}(x) + v\, h_m(x) \quad (6)$$

e. The final prediction of the model $\hat{y}$ is given after a number of iterations (M):

$$\hat{y} = F_m(x) = \sum_{m=0}^{M} v\, h_m(x) \quad (7)$$

In the equation above, it is considered that $h_0(x)$ is the initial prediction and also $F_m(x)$ is the ensemble model after m interactions, $h_m(x)$ is the new tree (learner) added at step m, v (nu) is the learning rate which is defined as a parameter that controls how much each new tree contributes to the final model.

In the first stage of our research, we simulated 10 wells exploiting polluted extraction area and the duration of decontamination through the four AI models.

After extracting an amount of 30 l/s for 700 hours, models predicted the following final pollution values:

- Model Training: 1. Linear Regression - Mean Absolute Error (MAE): 17.5347 mg/L
- Model Training: 2. Decision Tree - Mean Absolute Error (MAE): 9.8225 mg/L
- Model Training: 3. Random Forest - Mean Absolute Error (MAE): 7.9185 mg/L
- Model Training: 4. Gradient Boosting - Mean Absolute Error (MAE): 7.9163 mg/L

- Model Performance Summary

1. Linear Regression: MAE = 17.5347 mg/L
2. Decision Tree: MAE = 9.8225 mg/L
3. Random Forest: MAE = 7.9185 mg/L
4. Gradient Boosting: MAE = 7.9163 mg/L

The best model turned out to be Gradient Boosting, the actual data obtained being close to the predicted ones (Figure 2). Through this model we can also simulate the behavior of other water extraction wells in the area in the future (Figure 3).

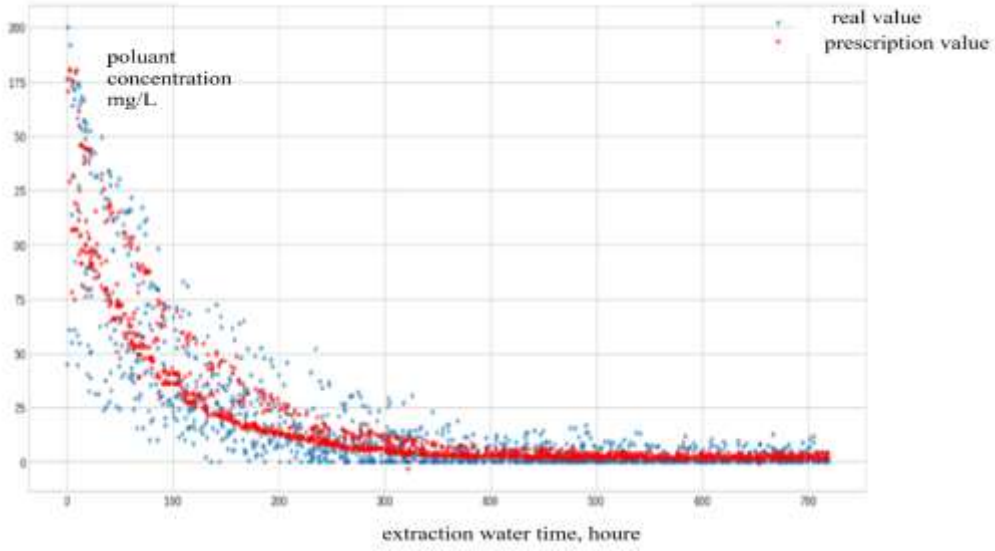

Figure 2. *AI Gradient Boosting Model Analysis*

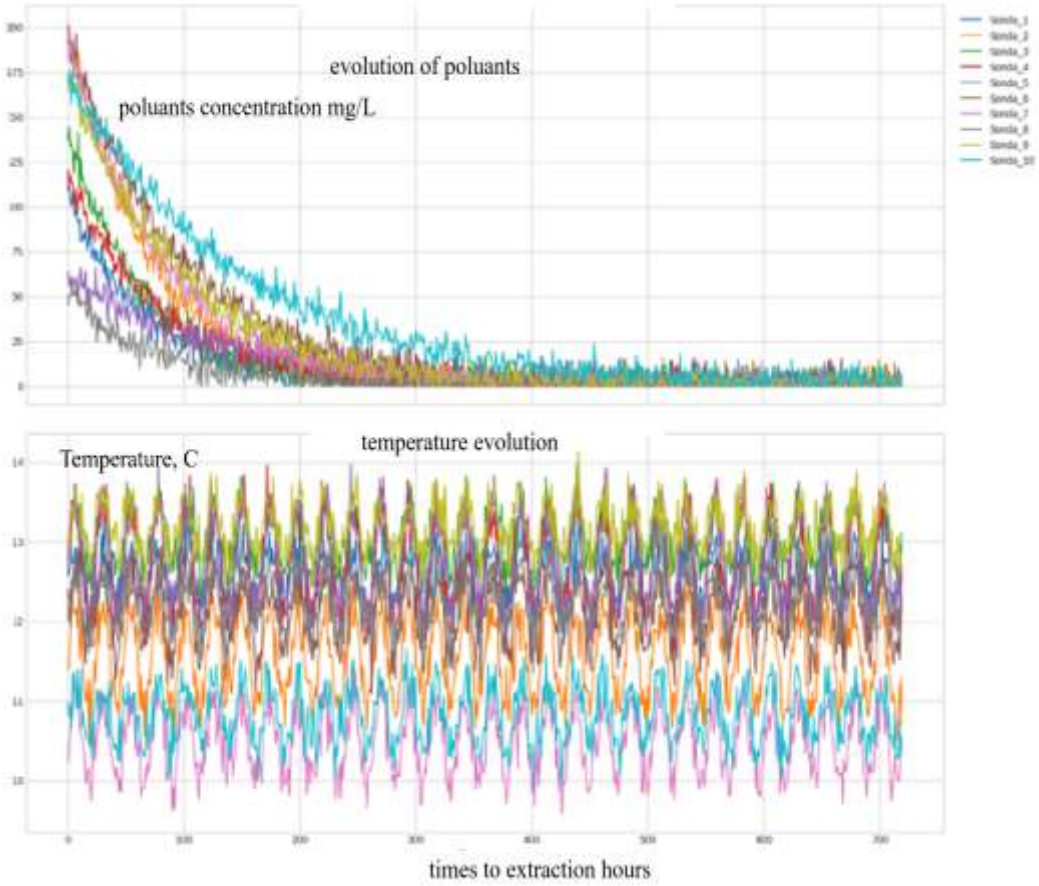

Figure 3. *AI Gradient Boosting Model Analysis (influence of pollutants on water temperature)*

In order to analyze the effect of pollutants on the temperature of the reservoir water, we studied a pollutant consisting of 50 mg/l gasoline (density 770 kg/m^3) and 75 g/l diesel with a density of 950 kg/m^3. This pollutant was degraded and was mixed with water (113 mg/liter). The simulation consisted of observing the effect of the pollutant on the temperature during extraction from the soil.

The formed solution was passed through a layer of gravel and extracted with a vacuum pump (Table 1).

Table 1. *Effect of the pollutant on the temperature of the extracted water*

Temperature, C°	**Pollutant concentration, mg/l**	**Extraction, hours**
y	x_1	x_2
12,93	112,27	0
12,92	109,42	1
12,85	108,09	2
12,73	102,59	3
12,72	101,97	4
12,71	100,49	5
12,68	98,64	6
12,59	94,98	7
12,57	92,23	8
12,44	90,86	9

The variation equations are:

a. Linear equation of temperature variation (y) as a function of concentration (x):

$$y = 45.613x - 478.85 \quad (8)$$

with R^2=0.968,

b. Logarithmic equation of temperature variation (y) as a function of concentration (x):

$$y = 579.21\ln(x) - 1371.6 \quad (9)$$

with $R^2 = 0.967$,

c. Polynomial equation of temperature variation (y) as a function of concentration (x):

$$y = 697095x^6 - 5E^{+07}x^5 + 2E^{+09}x^4 - 3E^{+10}x^3 + 3E^{+11}x^2 - 1E^{+12}x + 3E^{+12} \quad (10)$$

with $R^2 = 0.9988$,

d. Power equation of temperature variation (y) as a function of concentration (x):

$$y = 5E\text{-}05x^{5.7393} \quad (11)$$

with $R^2 = 0.9715$,

e. Exponential equation of temperature variation (y) as a function of concentration (x):

$$y = 0.3225e^{0.4519x} \quad (12)$$

with $R^2 = 0.972$,

It was also interesting to create an equation to simulate the temperature variation depending on the amount of pollutant extracted and the hours of extraction (Figure 4).

$$y = 10.69646 + 0.020083x_1 - 0.00275x_2 \quad (13)$$

with $R^2 = 0.96085$,

where:

- y is temperature of water, C°,
- x_1 represent pollutants concentration, mg/l,
- x_2 represent the extraction time (in hours).

Note: the flow was turbulent and it was intended not to be over long distances to limit temperature losses on the well extraction to the maximum.

We observe that there is a negative influence of the decrease in water temperature with the decrease in the concentration of pollutants in the mixture. The following research consisted in analyzing the influence of the change in extraction flow rates and pollutant concentration on the temperature of the extracted water.

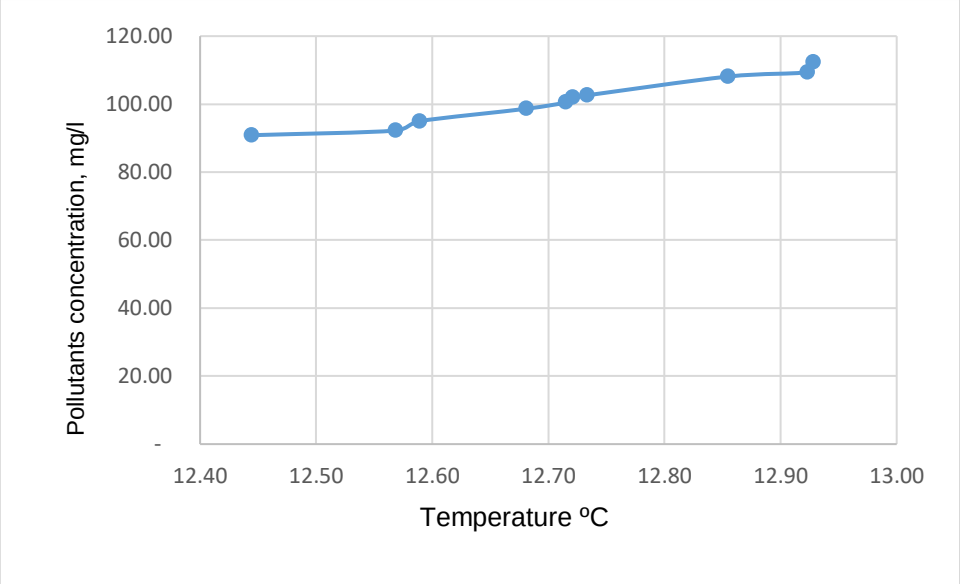

***Figure 4**. Influence of pollutant concentration on temperature*

We took an aquifer volume of 2,000,000 liters, an initial concentration of 50 mg/l gasoline and 75 gtl diesel and a simulation time of 120 days.

The flow rate was 25,000 liters per day in phase 1 and then 10,000 liters per day in phase 2 (after 40 days from the start of drilling).

In figure 5 we have plotted the variation of the pollutant concentration changes depending on the extraction flow rate (without mixing these two products).

The simulation found (as in practice) a degradation rate of 0.04 l/day for gasoline and 0.02 l/day for diesel.

In the case of mixing gasoline with diesel, a rate of 1 mg/l day is obtained for gasoline at a half-saturation rate of 15 mg/l and 40 mg/l inhibition constant of diesel on gasoline, and

for diesel, a rate of 0.5 mg/l day for diesel at a half-saturation rate of 30 mg/l and 20 mg/l inhibition constant of gasoline on diesel (figure 5).

The four simulation models in this case were of the K zero and K first type with a constant gasoline degradation rate of 0.4 mg/l day, the Haldane model with a specific gasoline degradation rate of 1.2 mg/l and the simple monod model.

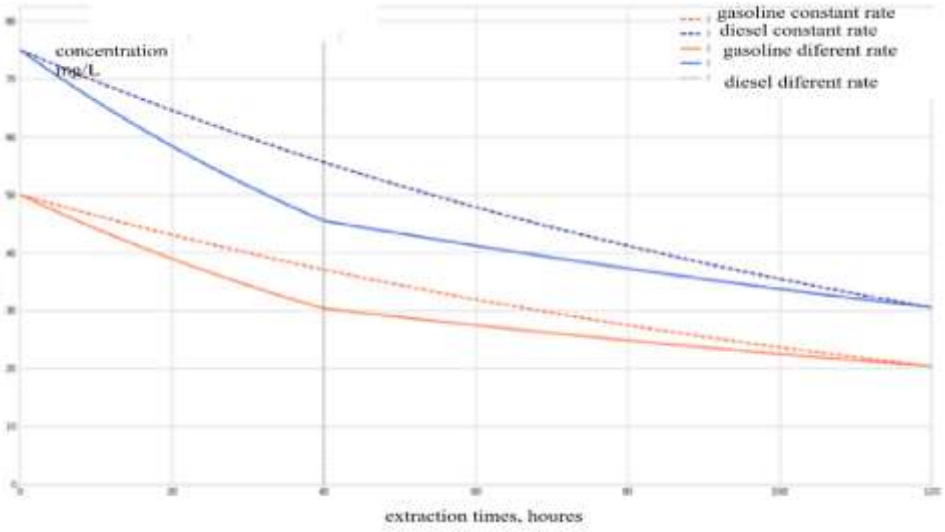

Figure 5. *Variation of pollutant concentration during extraction*

The zero-order model (Zero-Order Kinetics) starts from the theory that the pollutant degradation rate is constant over time, regardless of its concentration.

The reaction proceeds at the same rate until the pollutant is completely consumed, this model being applicable for the case of a limitation of the reaction rate by the presence of an enzyme.

Equation is [18]:

$$\frac{dC}{dt} = -k \tag{14}$$

where C is the pollutant concentration (mg/L) that is consumed over time (t-days) and k is a rate constant (mg/L days).

The First-Order Kinetics model is applicable for low concentrations and describes the rapid consumption of the pollutant, with the reaction rate decreasing over time.

The equation is of the form, [19]:

$$\frac{dC}{dt} = -k\,C \tag{15}$$

Where C is the pollutant concentration (mg/L) that is consumed over time (t-days) and k is a first-order rate constant (mg/L days).

The Monod model (Monod Kinetics) is fundamental to microbial growth and pollutant (substrate) consumption.

This model relates the degradation rate to the pollutant concentration in a nonlinear manner, at very low concentrations, the model behaving similar to the first-order model, [20].

At very low concentrations, the degradation rate reaches a maximum value and becomes concentration-independent (similar to zero-order behavior) as the microbial system becomes saturated, [21].

$$\frac{dC}{dt} = -\mu_{max}\frac{C}{K_s+C} \tag{16}$$

where C is the pollutant concentration (mg/L) consumed during (t-days), μ_{max} represents the maximum degradation rate (mg/L day) and K_s is a half-saturation constant which is thus the degradation rate of half the maximum value.

A low value indicates a high affinity of microorganisms for the pollutant.

The Haldane model (Andrews Haldane Kinetics) is a modification of the Monod model, which introduces a substrate inhibition term, being used to describe the degradation of substances that, at high concentrations, become toxic or inhibitory to the microorganisms responsible for degradation (such as phenols) [22].

At low and medium concentrations it behaves similarly to the Monod model (figure 6), but at high concentrations, the degradation rate starts to decrease due to the inhibition effect [23].

$$\frac{dC}{dt} = -\mu_{max}\frac{C}{K_s+C+\frac{C^2}{K_i}} \tag{17}$$

where C is the concentration of the pollutant (mg/L) that is consumed during (t-days), μ_{max} represents the maximum degradation rate (mg/L day), K_i is an inhibition constant (its low value makes the pollutant toxic) and K_s is a half-saturation constant which is thus the degradation rate of half the maximum value.

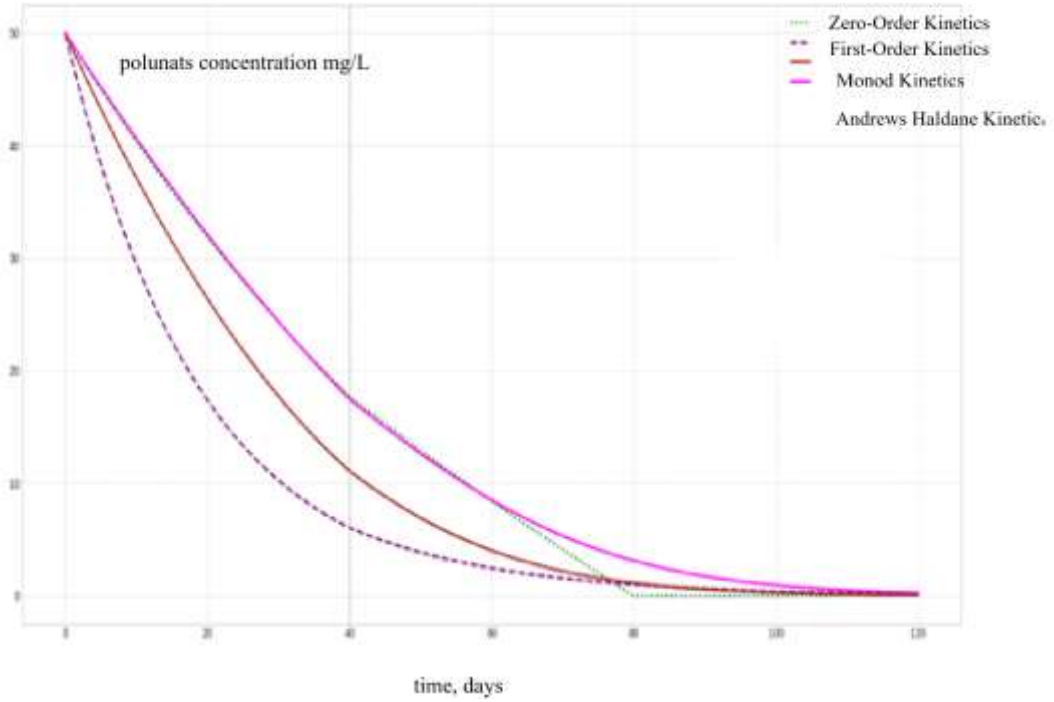

Figure 6. *Variation of pollutant concentration during degradation of gasoline pollutants with analysis of models*

RESULTS OF ANALYSIS

In the study conducted, we started from the project carried out within the investment described above. Following the monitoring of the operation of this system after one year, we simulated the thermal stress induced by the exploitation of groundwater [24].

Thus, in the first part, we analyzed the outlet temperature of the thermal water heating agent from the heat pump, as a function of the soil temperature measured when taking water and injecting water into the borehole and also as a function of the temperature of the heat pump inlet agent (the water from the well) [25].

In figure 7 we have shown the outlet temperature of the thermal water heating agent from the heat pump.

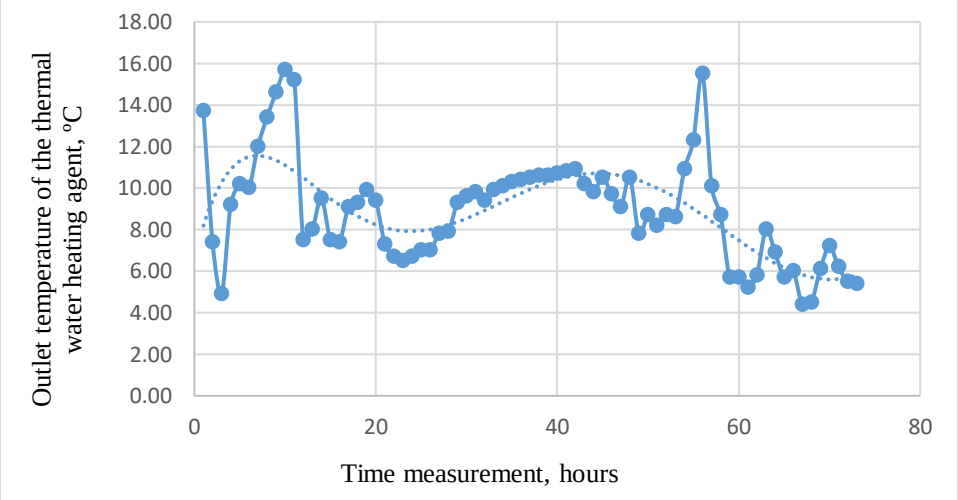

***Figure 7**. Variation of the outlet temperature of the thermal water heating agent from the heat pump (hourly variation)*

We note that we cannot write an equation for the variation of this temperature of the reservoir water (y), having a fairly large error (x is time to measurements).

$$y = -7E^{-09}x^6 + 2E^{-06}x^5 - 0.0002x^4 + 0.0092x^3 - 0.2044x^2 + 1.7432x + 6.6505 \quad (18)$$

with $R^2 = 0.4396$.

Also in figures 8, 9 and 10 we have shown the hourly variation of the temperature of the subsoil at the entrance to the heat pump, of the water at the entrance to the heat pump and of the soil at the exit from the heat pump.

A loss of almost 1 ºC is observed when passing through the heat pump and almost 4 ºC in the water injection area of the heat pump. In figure 11, we have analysed equation (18) and effects of the member to the equation.

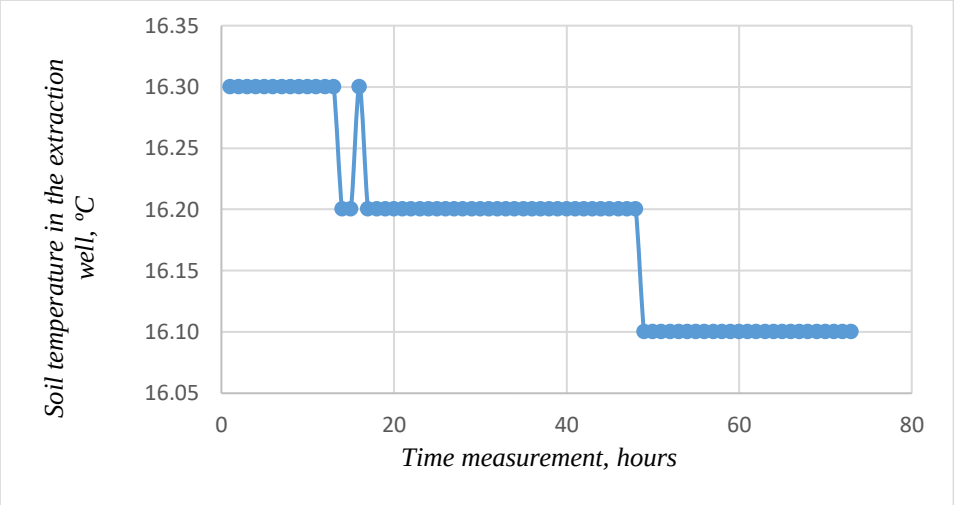

Figure 8. *Variation of subsoil temperature in the water extraction area (hourly variation)*

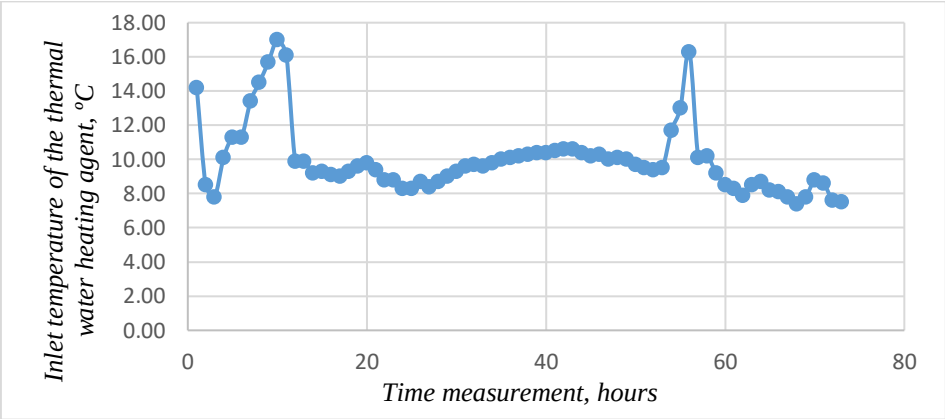

Figure 9. *Variation of the inlet temperature of the thermal water heating agent from the heat pump (hourly variation)*

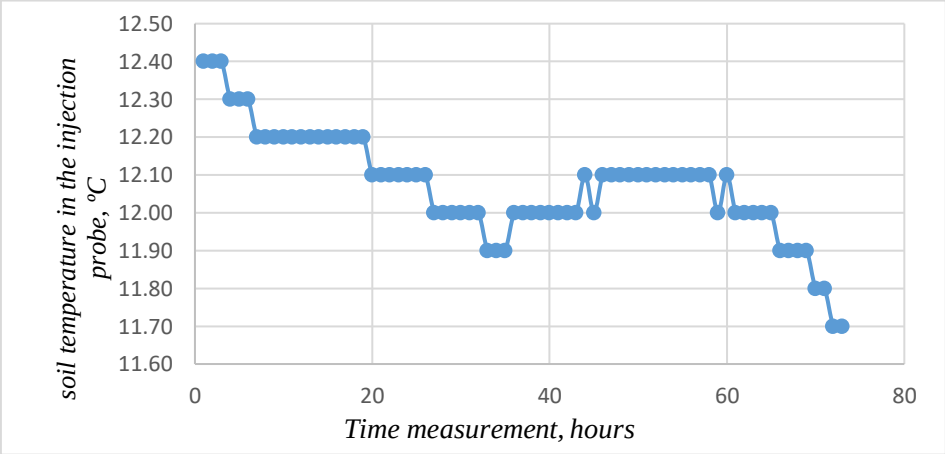

Figure 10. *Variation of the subsoil temperature in the water extraction area (hourly variation)*

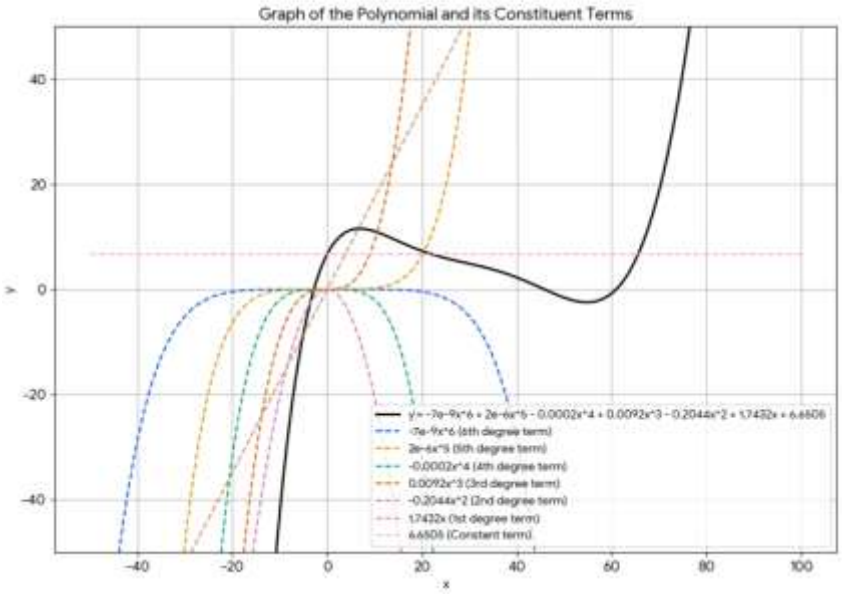

Figure 11. *Graph of equation 1 and impact of member equation*

In order to analyze the thermal efficiency of water extracted from the ground, we created a numerical relationship that provides us with data on the variation of the outlet temperature of the thermal water heating agent from the heat pump (y), as a function of the soil temperature measured when taking water and injecting water into the borehole (x_1 and x_2) and also as a function of the temperature of the heat pump inlet agent (the water from the well) (x_3).

The equation is of the form:

$$y = -51.0293 + 4.42327x_1 - 1.89612x_2 + 1.128339x_3 \quad (19)$$

with coefficient of determination R^2=0,84865.

The graphical modelling is shown in figures 12 and 13.

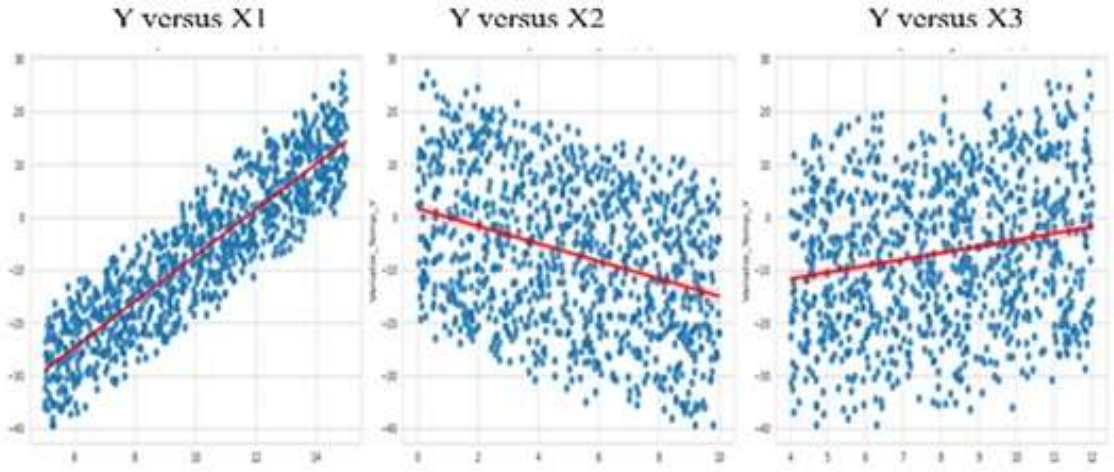

Figure 12. *Variation of the outlet temperature of the thermal water heating agent from the heat pump (y), depending on the soil temperature measured at water intake and water injection into the borehole (x_1 and x_2) and also depending on the temperature of the heat pump inlet agent (well water) (x_3)-data analysis*

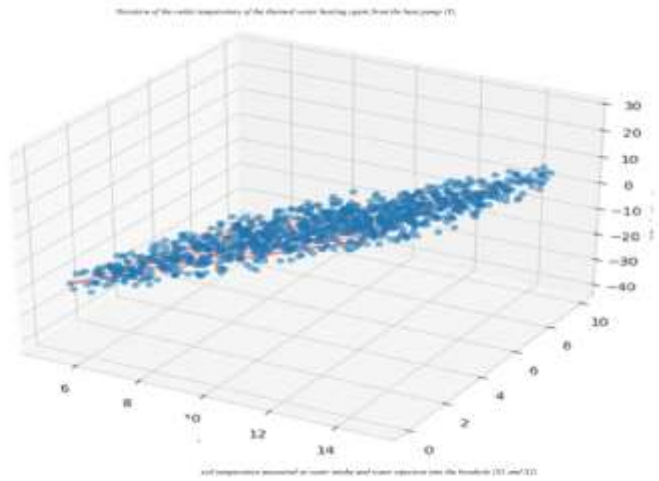

Figure 13. *Regression plot for soil temperature measured at water intake and water injection into the borehole (x_1 and x_2) and also as a function of the temperature of the heat pump inlet agent (well water) (x_3) - data analysis*

In what follows we studied AI development models as follows [11]:

a. Linear Regression:

MSE = 0.2379, and R^2 = 0.9988.

b. Ridge Regression:

MSE = 0.2378, and R^2= 0.9988.

c. Random Forest:

MSE = 1.8425, and R^2 = 0.9910.

d. Neural Network (MLP):

MSE = 0.3143, and R^2 = 0.9985.

* MSE (Mean Squared Error): The mean squared error. The lower the value, the better.

* R^2: Indicates how well the model explains the variation in the data. The closer to 1 the better.

EQUATIONS / STRUCTURE OF AI MODELS

Model: Linear Regression

$$y = -51.2210 + (4.4240\ x_1) - 1.8878\ x_2 + (1.1476\ x_3) \quad (20)$$

(We notice how close the AI coefficients are to those in the original equation).

Model: Ridge Regression

$$y = -51.2137 + (4.4234\ x_1) - 1.8875\ x_2 + (1.1473\ x_3) \quad (21)$$

(We notice how close the AI coefficients are to those in the original equation).

Model: Random Forest

This model does not have a simple algebraic equation. It is an ensemble of 100 decision trees. The final prediction is the average of the results of all the trees.

Model: Neural Network (MLP)

This model is a neural network and does not have a simple equation. Its architecture is:

- Input layer: 3 neurons (for $X1$, $X2$, $X3$),

- Hidden layers: (64, 32),
- Output layer: 1 neurone (for *Y*).

CONCLUSIONS

Following this analysis, we can conclude the following aspects of the thermal groundwater in the Petroleum-Gas University of Ploiesti area:

- The average water temperature is 8.92 ℃,
- The average basement temperature is 16.8 ℃,
- The average loss of basement temperature (due to water injection) is 6.33 ℃,
- The average loss of water temperature (due to use in the heat pump) is 4.11 ℃.

General characteristics of groundwater in the studied area are as follows:

- Estimated temperature: although public studies do not specify an exact water temperature at a certain depth, a reasonable estimate can be made. At depths of more than 20-30 meters, the temperature of the soil and groundwater tends to stabilize at a value close to the average annual air temperature in the locality. For Ploiesti, this is approximately 11-12°C. Therefore, it can be estimated that the water in medium-depth aquifers (50-150 m) has a constant temperature in this range, being ideal for use with heat pumps.
- Main aquifers: the Ploiesti area is rich in groundwater resources, the main catchment fronts for drinking water supply being "Crângul lui Bot", Ploiesti Nord-Vest and Ploiesti Nord-Est. These are important, deep aquifers, which confirm the presence of large volumes of underground waters.
- Contamination warning: some older studies mention that the (shallow) groundwater in the southern and southeastern areas of the municipality may be contaminated with petroleum products. This is an important factor to consider and requires a water quality analysis before designing an open geothermal system.

REFERENCES

[1] Allan, M.L., Kavanaugh, S.P., Thermal conductivity of cementitious grouts and impact on heat exchanger length design for ground source heat pumps, International Journal of HVAC&R Research, Vol. 5, (2), 1999.

[2] Allan, M.L., Philippacopoulus, A.J., Thermally Conductive Cementitious Grouts for Geothermal Heat Pumps, FY 1998 Progress Report, BNL 66103, 1998.

[3] Selim M.Y.E., Helali A.H.B., Thermal evaluation of some liquid coolants under real engine conditions. In: ASME international spring conference, ICED, Texas, San Antonio, USA; 2000.

[4] Bejan, A., Entropy generation through heat and fluid flow, John Wiley & Sons Inc., New York, 1992.

[5] Bini, R., Manciana, E., Organic Rankine Cycle Turbogenerators for Combined Heat and Power Production from Biomass. In: Proceedings of the 3rd Munich Discussion Meeting 1996, ZAE Bayern (ed.), Munich, Germany, 1996.

[6] Claesson, J., Eskilson P., Conductive Heat Extraction to a Deep Borehole, Thermal Analysis and Dimensioning Rules. Energy 13/6, 2024.

[7] http://hybridenergy.upg-ploiesti.ro/

[8] Neacsu, S., Trifan, C., Albulescu, M., Eparu, C., Ionescu, E.M., Analysis on energy available in soil to be used for heating dwelling places, CNEI, Bacău, 2005.

[9] Neacsu, S., Trifan, C., Albulescu, M., Răspunsul termic al solului în cazul utilizării pompelor de căldură, Conferinţa naţională de termotehnică cu participare internaţională, Ediţia XVI-a, Vol 2, Ploieşti, 2007.

[10] Cirjan D., Purghel I., Stoicescu M., Chis T., An energy efficiency model based on heat pumps of a public buılding with conventional heating, 4th International Scientific Research Congress, Istanbul, June 21-22, 2025, Congress Book, pp. 166-171. https://www.isracademy.org/

[11] Cirjan D., Purghel I., Stoicescu M., Chis T., A treatment and recovery of petroleum products extracted from polluted water, 4th International Scientific Research Congress, Istanbul, June 21-22, 2025, Congress Book, pp. 172-178. https://www.isracademy.org/

[12] Song G., St. John D., Corrosion behavior of magnesium in ethylene glycol. Corros Sci; 46:1381–99. 2004

[13] Mohamed M.A.M., Osman M.A., Potter T.L., Levin R.E., Lead and cadmium in Nile river water and finished drinking water in greater Cairo, Egypt. Environ Int., 24:767–72. 1998

[14] French CCJ. Problems arising from the water cooling of engine components. Inst Mech Eng., 184:507–30. 1969–1970

[15] Alcock JF. Thermal loading of diesel engines. Trans Inst Eng, 77. 1965

[16] Feidt, M., Thermodynamique et Optimisation Energétique de Systèmes et Procèdes, Technique et Documentation (Lavoisier), Paris, 2024

[17] Cheong S.K.A., The measurements of low concentration of dissolved gas in water. M.Sc. Thesis, University of Toronto; 1968.

[18] Incropera, F.P., David P. DeWitt, Fundamentals of Heat and Mass Transfer, John Wiley & Sons, New York, 1990.

[19] Lamb, H., Hydrodynamics, ed. a 6-a. Cambridge University Press, 1992 (Dover Publications, New York, 1925).

[20] Rybach, L., Sanner, B., Ground-Source heat pump systems the European experience, Institute of Applied Geosciences, Giessen, Germany.

[21] Sanner, B., Earth Heat Pumps and Underground Thermal Energy Storage in Germany, Proc. World Geothermal Congress: 2167-2172, 1995.

[22] Sanner, B., Prospects for Ground-Source Heat Pumps în Europe, Newsletter IEA Heat Pump Centre, 17/1, 1999.

[23] Sanner, B., Shallow Geothermal Energy, Justus-Liebig University, Giessen, Germany, GHC Bulletin, June 2001.

[24] Vidal, J., Thermodynamique - Méthodes appliquées au raffinage et au génie chimique, Edition Techniq, Paris, 1993.

[25] Bergles, A.E., Rohsenow, W.M., The determination of forced-convection surface-boiling heat transfer. ASME J. Heat Transf. 1, 365–372. 1964.

Received: August 2025; Revised: September 2025; Accepted: September 2025; Published: September 2025